

Experimental and theoretical study of the distance dependence of metal-enhanced fluorescence, phosphorescence and delayed fluorescence in a single system

Cite this: *Phys. Chem. Chem. Phys.*, 2013, **15**, 19538

Hirdyesh Mishra, Buddha L. Mali, Jan Karolin, Anatoliy I. Dragan and Chris D. Geddes*

Received 11th February 2013,
Accepted 20th September 2013

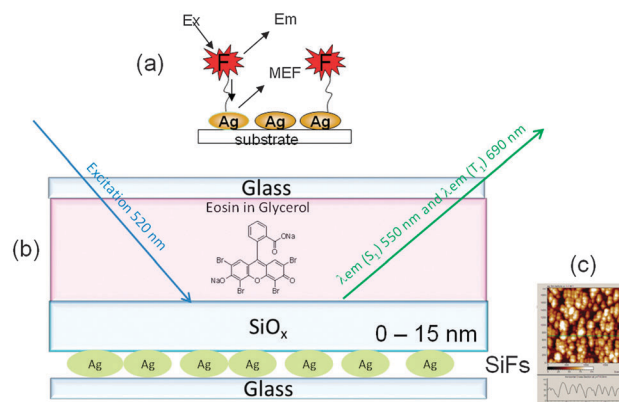
DOI: 10.1039/c3cp50633a

www.rsc.org/pccp

Distance dependent singlet and triplet metal-enhanced emission of eosin from silica coated silver island films (SiFs) has been studied by steady-state and time resolved fluorescence techniques, along with theoretical finite difference time domain (FDTD) numerical simulations, to understand how the thickness of the dielectric coating surrounding silver nanoparticles fundamentally affects luminescence enhancement. Our findings suggest that the distance dependence of metal-enhanced phenomena such as fluorescence, phosphorescence and delayed fluorescence is underpinned by the decay of the electric near-field, and depending on the actual silver silica sample embodiment, one can see either decreased or enhanced luminescence. These results not only expand our current MEF thinking but also suggest that one may well be able to approximate plasmon-enhanced luminescence values.

1.0 Introduction

The deposition of silver metal and subsequently silver island films (SiFs – sub-wavelength size silver nanoparticles formed by reduction of silver nitrate on a glass surface) has become a useful method for studying plasmon-enhanced phenomena from the visible to the near-infrared spectral range. Under suitable conditions, the close proximity of fluorophores to metal particles *i.e.* near-field interactions, allows for dramatic effects on fluorescence intensity, photo-stability and lifetimes. Geddes and coworkers^{1–13} have developed a mechanistic interpretation of these near-field effects, as well as numerous applications of MEF itself. The current interpretation of MEF is underpinned using a model whereby non-radiative energy transfer occurs from excited fluorophores (dipoles) to surface plasmons in non-continuous films, as shown in Scheme 1. The surface plasmons in turn efficiently radiate the emission of the coupled fluorophores, *i.e.* radiate the coupled quanta. This interpretation has also led to the further development of metal enhanced chemiluminescence,^{14,15} metal-enhanced phosphorescence,^{16–18} and the discovery of plasmonic electricity by the Geddes group.^{19,20}



Scheme 1 (a) Current interpretation of metal-enhanced fluorescence, (b) cartoon depicting the sample geometry used to study the distance dependence of MEF for S_1 and α - S_1 emission from eosin in glycerol on SiO_2 coated SiFs (silver island films). (c) AFM images of a SiFs film deposited on a glass slide.

Silver surfaces can be reactive and the photodegradation of absorbed species is a common occurrence when probed using electromagnetic radiation. Thus, SiF surfaces can be readily protected in such a way that they maintain their ability to enhance luminescence. It is therefore important to study the distance dependent decay of the electrical field around SiFs/nanoparticles and its propagation in the spacer medium, and how this decay ultimately affects luminescence enhancing properties. In earlier studies, the distance dependence of fluorescence

The Institute of Fluorescence and Department of Chemistry & Biochemistry,
University of Maryland Baltimore County, 701 East Pratt Street, Baltimore, MD,
21202, USA. E-mail: geddes@umbc.edu; Fax: +1-410-576-5722;
Tel: +1-410-576-5723

quenching and enhancement of fluorophores close-to various metallic surfaces was studied. In these reports, the major thrust was the dependence of the *emission rate* on the distance between the dye layer and the metallic surface where the emission is thought to be quenched due to dipole damping when molecules are adsorbed directly on the surface.²¹ Another consideration is the enhanced fluorescence due to increased electromagnetic fields and the plasmon coupling mechanism.²² The enhancement of fluorescence intensity generally depends on the surface features (density of nanoparticles, shape and size, *etc.*) and the distance and dipole orientation of fluorophores from/to the surface.²²

Different fluorescence enhancement factors have been reported by several workers in their distance-dependence MEF studies. Nearly 5- to 12-fold enhancements in fluorescence intensity for 20 to 25 nm fluorophore–metal distances were reported for a metal core–silica-spacer colloidal particle system.^{23–28} Lakowicz and coworkers,^{29–33} have reported a 10 nm distance for maximum fluorescence enhancement of fluorophores from SiFs using Langmuir–Blodgett films in which below 10 nm fluorescence quenching has been reported due to nonradiative energy transfer. Distance dependent oscillatory fluorescence enhancement functions and decay rates of fluorophore or luminophore from SiFs have also been reported by many other researchers in the past.^{34,35} In a recent study of the distance-dependence of fluorescence enhancement, in contrast to the quenching near metallic surfaces, a maximum enhancement was reported from the contact with a metallic surface and a photonic crystal.^{36,37} To understand these somewhat contradictory results, we have undertaken detailed systematic studies of the distance dependent near-field effects on the photophysics of the eosin molecule close-to silver nanostructures, through fluorescence spectroscopic techniques and finite difference time domain (FDTD) numerical calculations, controlling the precise distance from 1 to 15 nm.

Eosin is a red xanthene dye resulting from the reaction of bromine on fluorescein. Due to the heavy atom effect, it shows delayed fluorescence (α -S₁ → S₀) and phosphorescence (T₁ → S₀) at room temperature, along with traditional fluorescence (S₁ → S₀) in the wavelength range 475 to 800 nm.^{38,39} The population of the excited singlet state (S₁) by thermal activation of the triplet state (T₁) is responsible for E-type delayed fluorescence. Due to its long decay time, delayed fluorescence has been widely used to investigate the rotational diffusion time of biological macromolecules in membranes and also to characterize metal oxide surfaces.¹⁵ Eosin is used to stain cytoplasms, collagen and muscle fibers for microscopic examination. Further it is also used for dyeing textiles, ink manufacturing, for coloring cosmetics, for coloring gasoline and as a toner, to name but just a few applications. Due to the potential uses of eosin in biology⁴⁰ and industrial research,⁴¹ distance dependent MEF studies of eosin will be helpful to develop intense fluorescent probes in the future for studying systems in different temporal ranges *i.e.* from nano- to millisecond time range. Zhang *et al.*⁴² have reported on a 2-fold enhancement in singlet–triplet emission of eosin in 4% wt polyvinyl alcohol films coated on SiF surfaces in temperature dependent studies. However in this manuscript, we have obtained

~9-fold enhancement in fluorescence (S₁ → S₀) and a nearly 4-fold enhancement in delayed fluorescence (α -S₁ → S₀) and phosphorescence (T₁ → S₀) of eosin in anhydrous glycerol close-to SiO_x-SiFs with respect to a control sample containing no silver (Scheme 1), with a nearly 20-fold enhancement of fluorescence and a 7-fold enhancement in both triplet and delayed emission observed close-to silver nanoparticle coated glass slides. Our findings are not only helpful for understanding the distance dependence dynamics of fluorophores from SiFs, but also for the numerous practical applications that enhance fluorescence and phosphorescence yield for the next generation energy efficient materials, as biosensors, photonic devices and MEF based assay platforms. To the best of our knowledge, this is the first report showing the distance dependence of all 3 luminescence decay routes.

2.0 Experimental section

2.1 Materials

Eosin, silane-prep glass microscope slides, silver nitrate (99.9%), sodium hydroxide (99.996%), ammonium hydroxide (90%), D-glucose, ethanol (HPLC/spectrophotometric grade) and anhydrous glycerol were purchased from Sigma-Aldrich Chemical company (Milwaukee, WI, USA). The SiFs were prepared according to previously published procedures.^{6–9} Twenty micro-liters of eosin in glycerol [10^{−3} M] was sandwiched between both glass and the SiF coated silane prep slides, respectively. Different thin layers of SiO_x on SiFs were prepared using an Auto 306 Vacuum coater (AccuCoat Inc., Rochester, NY, USA). The thickness of the deposited film was monitored using a quartz crystal microbalance.

2.2 Instrumentation

Absorption spectra of acriflavine on blank glass substrates and SiFs containing PVA polymer films were collected using a single beam Varian Cary 50-Bio UV-vis spectrophotometer. Emission spectra were collected using a Varian Cary Eclipse fluorescence spectrophotometer having a pulsed xenon arc source for excitation. A front-face sample geometry was used to undertake all the fluorescence measurements with a slit width of 5 nm, both in the excitation monochromator and emission monochromator channels. Fluorescence decays were measured using a HORIBA Jobin Yvon Fluoromax-4 and Temp-Pro fluorescence lifetime system employing the time-correlated single photon counting (TCSPC) technique, using a R928 and TBX-04 picosecond detection module. The excitation source was a pulsed LED source of wavelength 372 nm having maximum repetition rate 1.0 MHz and pulse duration 1.1 nanosecond (FWHM). The intensity decays were analyzed using decay analysis software (DAS) version 6.4 in terms of the multi-exponential model: $I(t) = \sum_i \alpha_i \exp(-t/\tau_i)$ where α_i are the amplitudes and τ_i are the decay times, $\sum_i \alpha_i = 1.0$. The values of α_i and τ_i were determined using nonlinear least squares impulse deconvolution analysis with the goodness of fit judged using the residual, autocorrelation

function and χ^2 values. The measurement error in decay time analysis was in the order of 0.01 ns.

3.0 Results and discussion

SiFs are sub-wavelength size silver nanoparticles formed by reduction of silver nitrate on a glass surface by a wet deposition method.^{1–3} Fig. 1 shows the absorption spectra of SiFs and SiFs coated with different thicknesses of SiO_x. SiFs typically show structured absorption, a maximum at 390 nm along with a band at 420 nm as shown in [Fig. 1(i)]. When quartz [SiO_x]

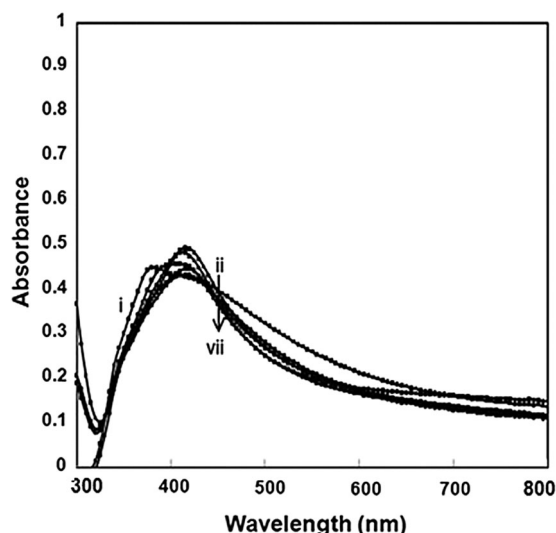


Fig. 1 Absorption spectra of SiFs coated with different thicknesses of SiO₂ (i) SiFs, (ii) 1 nm, (iii) 3 nm, (iv) 6 nm, (v) 9 nm, (vi) 12 nm and (vii) 15 nm SiO₂ coated on SiFs.

layers are coated onto SiFs deposited slides, the structured absorption of SiFs disappears, and a new red shifted band is readily observed at 400 nm. Further, upon increasing the thickness of the SiO_x layer, the optical density of the 400 nm band decreases [shown in Fig. 1(ii–iv)]. The extinction spectra of SiFs are the combinations of both absorption (Fig. 1) and scattering spectra. In these nanoparticle films, the absorption component is generally blue shifted and weak, while the scattering component is strong and red shifted.

The absorption spectra of eosin in glycerol [10^{-4} M] located between two glass slides is shown in Fig. 2a. It shows an absorption maximum at 525 nm with an optical density maximum ≈ 0.45 . On SiFs, the optical density increases up to 0.65 and it further increases for a 1 nm SiO_x coated film (~ 0.82). On further increasing the thickness of the SiO_x layer, the optical density decreases. The variation of enhancement in optical density of eosin on different optical density SiFs (0.45 to 0.50) coated with different thicknesses of SiO_x is shown in Fig. 2b, where the average of the absorbance of eosin was found to be maximum for 1 nm SiO_x coated SiFs. These results indicate that when a fluorophore is placed close-to metal nanostructures, the often strong localized electromagnetic field around the metallic particles subsequently increases and the rate of absorption subsequently increases, particularly for the 1 nm sample. In essence, conducting metallic particles can modify the free-space absorption condition in ways that increase the incident electric field felt by a fluorophore, *i.e.* an enhanced absorption cross-section.

Fig. 3a and b show the corresponding emission spectra of eosin from singlet and triplet states respectively. Eosin shows fluorescence [$S_1 \rightarrow S_0$] and delayed fluorescence [$\alpha\text{-}S_1 \rightarrow S_0$] maximum at ~ 550 nm and phosphorescence [$T_1 \rightarrow S_0$] maximum at ~ 690 nm respectively. We can see that eosin fluorescence enhances about 5.5 times (as compared to the control sample),

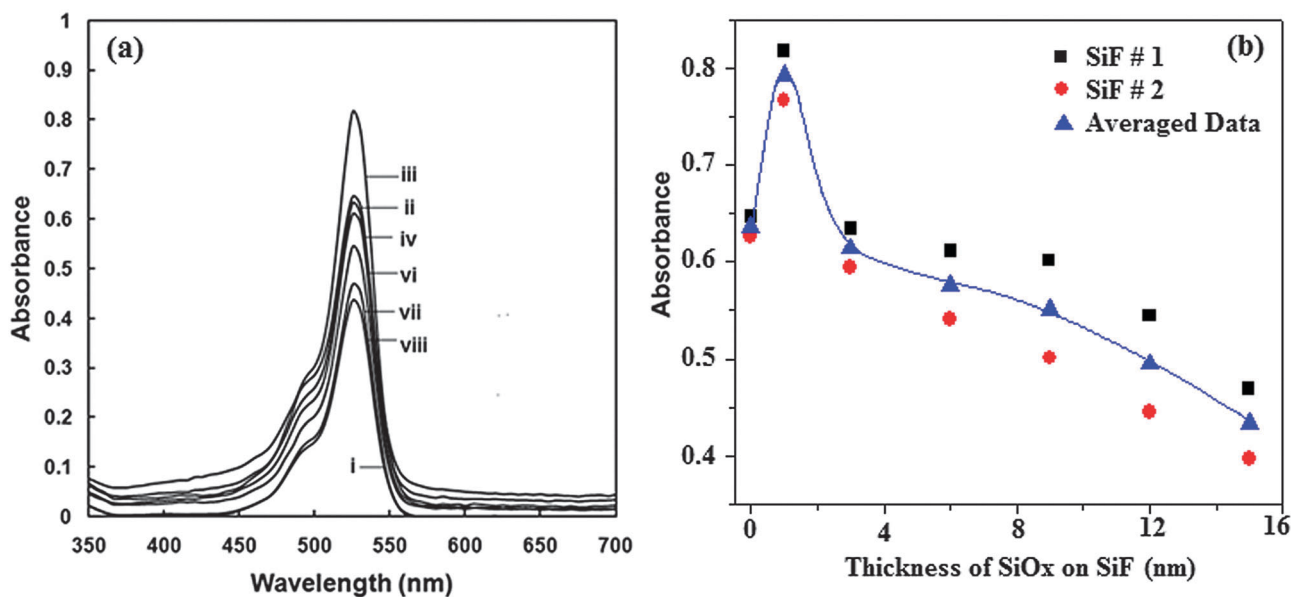


Fig. 2 (a) Absorption spectra of eosin (10^{-4} M) in glycerol on different thicknesses of SiO₂ coated SiFs. (i) Glass, (ii) SiFs, (iii) 1 nm, (iv) 3 nm, (v) 6 nm, (vi) 9 nm, (vii) 12 nm and (viii) 15 nm SiO₂ coated on SiFs. (b) Optical density of eosin on SiFs coated with different thicknesses of SiO₂.

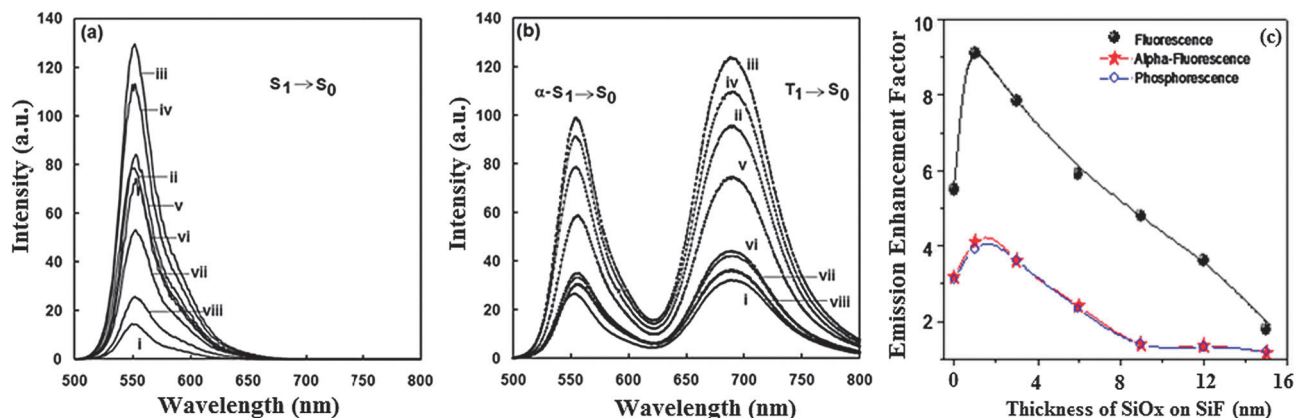


Fig. 3 (a) Fluorescence $S_1 \rightarrow S_0$, (b) delayed fluorescence $\alpha\text{-}S_1 \rightarrow S_0$ and phosphorescence $T_1 \rightarrow S_0$ spectra of eosin (10^{-4} M) in glycerol on different thicknesses of SiO_2 coated SiFs. (i) Glass, (ii) SiFs, (iii) 1 nm, (iv) 3 nm, (v) 6 nm, (vi) 9 nm, (vii) 12 nm and (viii) 15 nm SiO_2 coated on SiFs. (c) Enhancement factor (E.F.) of eosin (i) fluorescence, (ii) alpha fluorescence and (iii) phosphorescence from SiFs coated with different thickness of SiO_2 . E.F. – defined as the emission from the silvered substrate divided by that from an unsilvered otherwise identical control sample.

while delayed fluorescence and phosphorescence enhances about 3.0 times on SiFs. Further it is interesting that the intensity of both the singlet and triplet emission again increases in the presence of a 1 nm SiO_x layer, but upon further increasing the thickness of the protecting SiO_x layer, the enhancement of the singlet and triplet emission decreases, following the trend in optical density with thickness of SiO_x as shown in Fig. 2b. The enhancement factors for all the three emissions are shown in Fig. 3c, where enhancement factors are defined as the emission from the silvered substrate divided by that from an unsilvered otherwise identical control sample. These results indicate that the enhanced near-field absorption has a significant bearing on enhanced luminescence photophysics.

To further understand the fluorescence dynamics of the singlet and triplet states of eosin close-to the SiFs, decay time measurements were undertaken very carefully with different layers of SiO_x , and the time resolved results tabulated in Table 1. The fluorescence of the eosin molecule decays single exponentially with a decay time of 2.65 ns in glycerol measured in between the two glass slides, which similarly has been observed previously by Fleming *et al.*³⁸ It is interesting to note that the fluorescence decay of eosin becomes a double exponential with decay times 2.31 ns and 0.05 ns. The amplitude of the longer decay time is 70% while the decay amplitude of the shorter decay time is nearly 30%. Further decreases in magnitude of both decay

components is observed for a 1 nm layer of SiO_x , while the magnitude of both the decay times increases with an increase in the thickness of the SiO_x as shown in Fig. 4a. The change in longer decay time (τ_F) with the change in thickness of the protecting layer is shown in Fig. 4b. We can see that the magnitude of the decay values shows a decrease with the 1 nm layer of SiO_x , and then further increases with an increased distance from the SiFs. Further, we have also observed a decrease in delayed fluorescence decay time $\tau_{\alpha F}$ on SiFs ~ 3.28 ms for the eosin dye molecule close-to silver as compared to glass ~ 4.71 ms and a decrease in phosphorescence decay time τ_P on SiFs ~ 3.88 ms close-to silver is observed as compared to glass ~ 6.80 ms. The magnitude of both the decay values shows a decrease with the 1 to 3 nm layer of SiO_x , and then further increases with an increased distance from the SiFs similar to the fluorescence decay as shown in Fig. 4b. The metal enhanced phosphorescence decay time is shorter, as expected, than the metal-enhanced delayed fluorescence lifetime. These findings are consistent with our previously reported findings and trends for MEF^{7–15} and MEP.^{16–18}

Subsequently in this work, 2D theoretical finite-difference time-domain (FDTD) simulations were also undertaken using Lumerical FDTD Solution software (Vancouver, Canada) to study the near-field relative electric field intensities and distributions around silver nanoparticles (NP), and to study how the E -field effect correlates with the observed changes in the distance dependence of metal enhanced fluorescence (MEF) for the Ag- SiO_x sample embodiments. The simulation region was set to $600 \times 600 \text{ nm}^2$ with high mesh accuracy. To minimize simulation times and maximize the resolution of field enhancement around the metal particles, a mesh override region was set to 0.1 nm. The overall simulation time was set to 100 fs; calculations were undertaken over the wavelength range 300 to 600 nm. In these simulations the incident field is defined as a plane wave with a wave-vector that is normal to the injection surface (depicted as a white arrow in Fig. 5) and the scattered and total fields are monitored during the simulation such that the total or scattered transmission can be measured. Further,

Table 1 Time-resolved fluorescence decay parameters of eosin

Sample	τ (ns) [$S_1 \rightarrow S_0$]	τ (ms) [$\alpha\text{-}S_1 \rightarrow S_0$]	τ (ms) [$T_1 \rightarrow S_0$]	χ^2 [S_1]	χ^2 [αS_1]	χ^2 [T_1]
Glass	2.65 ± 0.02	4.71 ± 0.04	6.80 ± 0.02	1.461	1.373	1.299
SiFs	2.31 ± 0.06	3.28 ± 0.03	3.88 ± 0.03	1.211	1.377	1.062
1 nm SiO_2	2.20 ± 0.01	3.01 ± 0.03	3.25 ± 0.04	1.181	1.435	1.121
3 nm SiO_2	2.40 ± 0.02	2.8 ± 0.02	3.28 ± 0.05	1.341	1.381	1.135
6 nm SiO_2	2.47 ± 0.03	3.45 ± 0.04	4.37 ± 0.03	1.242	1.242	1.168
9 nm SiO_2	2.45 ± 0.03	3.97 ± 0.03	5.09 ± 0.03	1.168	1.148	1.164
12 nm SiO_2	2.47 ± 0.02	4.29 ± 0.04	5.41 ± 0.02	1.612	1.151	1.180
15 nm SiO_2	2.47 ± 0.01	4.75 ± 0.01	5.71 ± 0.02	1.311	1.176	1.181

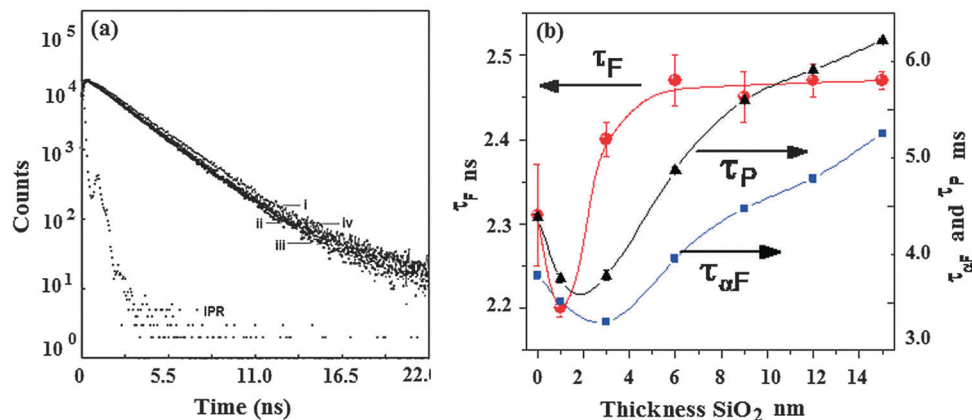


Fig. 4 (a) Decay curves of the fluorescence of eosin (10^{-4} M) in glycerol (i) on a glass slide, (ii) on SiFs, (iii) 1 nm SiO₂ coated on SiFs and (iv) 3 to 15 nm SiO₂ coated on SiFs (b) variation of decay time components of eosin (i) fluorescence, (ii) alpha fluorescence and (iii) phosphorescence from SiFs coated with different thicknesses of SiO₂.

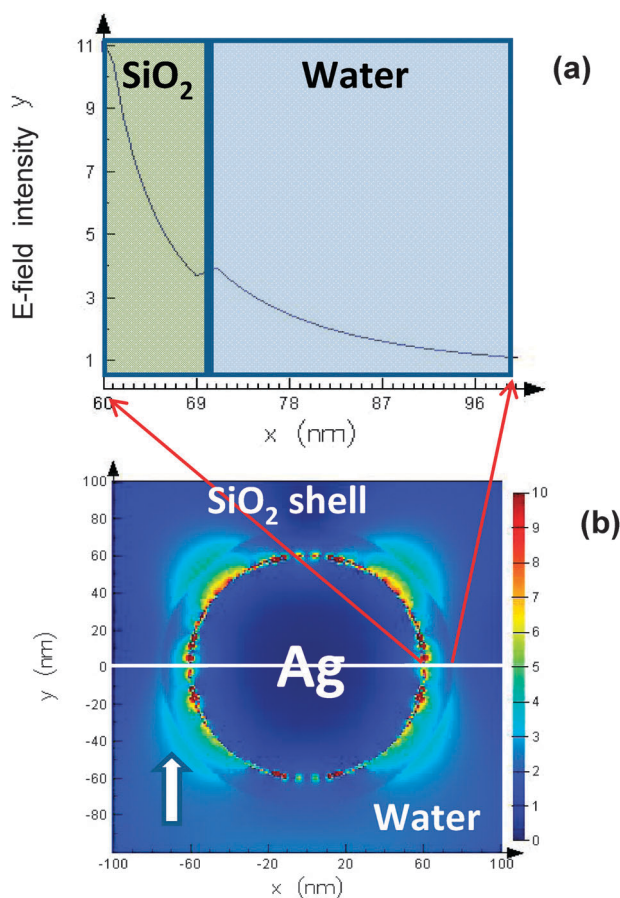


Fig. 5 (a) Decay of the E -field intensity upon the distance from a Ag-NP. The E -field was calculated from the 2D FDTD simulation for the system: the 120 nm silver core of the nanoparticle is covered with an SiO₂ shell of 10 nm thickness. (b) The 2D distribution of the E -field around the NP. Arrow shows the direction of incident light at a 400 nm wavelength. Red arrows show the axis along which the E field intensity was calculated [NP – nanoparticles].

distributions of E -fields around different layers of SiO_x coated silver nanoparticles and their extinction cross-section upon intensity of the incident light were also undertaken to rationalize the distance dependence E -field propagation around nanoparticles.

The decay of the E -field intensity as a function of distance from a Ag-NP is shown in Fig. 5a. The E -field was simulated for a 120 nm silver core nanoparticle covered with a SiO₂ shell of 10 nm thickness. Fig. 5b shows the 2D distribution of the E -field around the NP. While the white arrow shows the direction of incident light injection, the red arrows show the axis along which the E intensity was calculated (see Fig. 5a). Fig. 6a shows that the E -field on the silver surface increases almost 2-fold upon depositing SiO₂ which we attribute to the change in polarity and reflective index of the NP's environment, while on the surface of

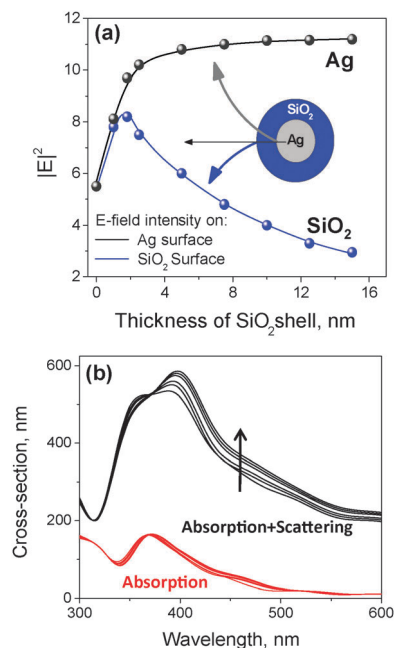


Fig. 6 (a) The E -field on the silver surface increases almost 2-fold upon depositing SiO₂ on the nanoparticle surface, i.e. upon the change of polarity of the NP environment, while on the surface of a glass shell the intensity of the E -field increases and then decays with the distance (glass thickness) from the Ag-NP surface. (b) Extinction and absorption spectra of a Ag-NP covered with glass of different thicknesses, from 0 to 15 nm. Plasmon scattering component of silver NP extinction spectra increases upon thickening of the SiO₂ shell.

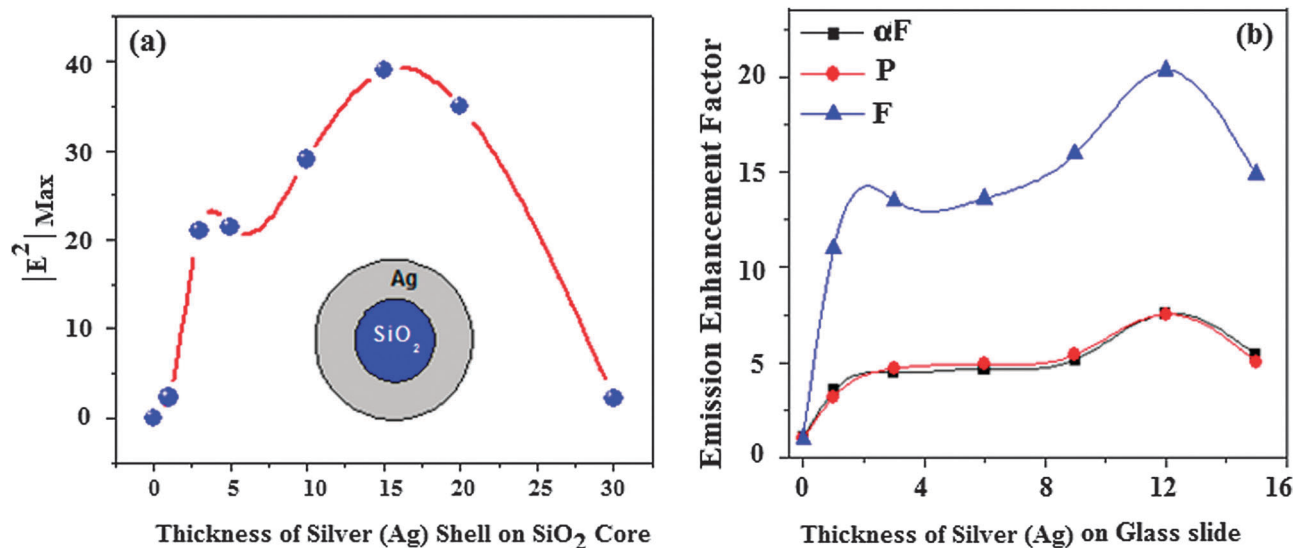


Fig. 7 (a) Distance of the near field intensity around a NP (core glass (SiO_x) 120 nm) upon thickening of the silver shell for a wavelength of 468 nm. (b) Enhancement factor (E.F.) of eosin (i) fluorescence, (ii) alpha fluorescence and (iii) phosphorescence experimentally determined from silver coated at different thickness on the glass slide. E.F. – defined as the emission from the silvered substrate divided by that from an unsilvered otherwise identical control sample.

the glass shell the intensity of the E -field increases and then decays with distance. Interestingly, the plasmon scattering component of the silver NP extinction spectra (Fig. 6b) increases upon thickening of the SiO_2 shell. These results are in very good agreement with the experimental observations as shown in Fig. 1. To further understand E -field enhancements, FDTD calculations were also undertaken for the *inverse sample embodiment*. These results indicate that maximum MEF will occur for a system having a 10 to 20 nm silver layer on 120 nm SiO_x Fig. 7a. These results are also in very good agreement with the associated experimental findings of MEF,⁴³ but surprisingly, no initial decrease in luminescence is observed as in Fig. 6a for the alternative samples embodiment, Fig. 7b. This suggests that the numerous reports of decreased fluorescence of SiO_2 coated Ag, may well be simply reflecting decreased electric field intensity, as compared to reports of close range fluorescence quenching.^{1,5,22}

Finally, it is notable that the enhanced fluorescence, phosphorescence and delayed fluorescence intensities follow the distribution of near-field intensity, suggesting that near field enhancement may to some degree be predicted using numerical simulations, even for molecules exhibiting complex photophysics such as eosin. To the best of our knowledge this is the first paper describing the distance dependence of luminescence enhancement on the emissive states from within the same system.

4.0 Conclusions

The distance dependence of the singlet and triplet character of eosin from the silver nano-structured material (SiFs) was undertaken using different spacer layers of SiO_x . A 1 nm layer of SiO_x was found to yield maximum absorption, singlet and triplet emission enhancement along with a corresponding maximum decrease in luminescence decay time. Further a very good correlation was observed in these experimental findings with

theoretical FDTD numerical simulations. Surprisingly, the FDTD results suggest that a decrease in emission below 1 nm is due to a change in the microenvironment/refractive index of the SiO_x layer and *not due to quenching* of the fluorophore, as reported by others.¹ Further, on comparing these results with the distance dependence of fluorescence for different layers of metal on glass, it appears that the maximum enhancement occurs for a 15 to 20 nm silver layer. Subsequently, our findings suggest that a 15 to 20 nm silver layer coated with 1–2 nm of SiO_x would yield a modestly enhancing surface for potential applications in surface bioassays.

Acknowledgements

The authors acknowledge the Institute of Fluorescence, (IoF) and the Department of Chemistry and Biochemistry at the University of Maryland Baltimore County (UMBC), USA, for salary support.

References

- 1 C. D. Geddes and J. R. Lakowicz, *J. Fluoresc.*, 2002, **12**, 121–129.
- 2 K. Aslan, S. N. Malyn and C. D. Geddes, *J. Fluoresc.*, 2007, **17**, 7–13.
- 3 K. Aslan, J. R. Lakowicz, H. Szmazinski and C. D. Geddes, *J. Fluoresc.*, 2004, **14**, 677–679.
- 4 K. Aslan, R. Badugu, J. R. Lakowicz and C. D. Geddes, *J. Fluoresc.*, 2005, **15**, 99–104.
- 5 K. Aslan, I. Gryczynski, J. Malicka, E. Matveeva, J. R. Lakowicz and C. D. Geddes, *Curr. Opin. Biotechnol.*, 2005, **16**, 55–62.
- 6 K. Aslan and C. D. Geddes, *Anal. Chem.*, 2009, **81**, 6913–6922.

- 7 K. Aslan, J. Huang, G. M. Wilson and C. D. Geddes, *J. Am. Chem. Soc.*, 2006, **128**, 4206–4207.
- 8 K. Aslan, P. Holley and C. D. Geddes, *J. Immunol. Methods*, 2006, **312**, 137–147.
- 9 K. Aslan and C. D. Geddes, *Plasmonics*, 2009, **4**, 267–272.
- 10 Y. Zhang, K. Aslan, M. J. R. Previte and C. D. Geddes, *Proc. Natl. Acad. Sci. U. S. A.*, 2008, **105**, 1798–1802.
- 11 A. I. Dragan, B. Mali and C. D. Geddes, *Chem. Phys. Lett.*, 2013, **556**, 168–172.
- 12 J. O. Karolin and C. D. Geddes, *J. Fluoresc.*, 2012, **22**, 1659–1662.
- 13 A. I. Dragan, E. S. Bishop, J. R. Casas-Finet, R. J. Strouse, J. McGivney, M. A. Schenerman and C. D. Geddes, *Plasmonics*, 2012, **7**, 739–744.
- 14 K. Aslan and C. D. Geddes, *Chem. Soc. Rev.*, 2009, **38**, 2556–2564.
- 15 M. H. Chowdhury, K. Aslan, S. N. Malyn, J. R. Lakowicz and C. D. Geddes, *Appl. Phys. Lett.*, 2006, **88**, 173104.
- 16 Y. X. Zhang, K. Aslan, S. N. Malyn and C. D. Geddes, *Chem. Phys. Lett.*, 2006, **427**, 432–437.
- 17 Y. X. Zhang, K. Aslan, M. J. R. Previte, S. N. Malyn and C. D. Geddes, *J. Phys. Chem. B*, 2006, **110**, 25108–25114.
- 18 M. J. R. Previte, K. Aslan, Y. X. Zhang and C. D. Geddes, *Chem. Phys. Lett.*, 2006, **432**, 610–615.
- 19 Y. X. Zhang, K. Aslan and C. D. Geddes, *J. Fluoresc.*, 2009, **19**, 363–367.
- 20 A. I. Dragan, Y. X. Zhang and C. D. Geddes, *J. Fluoresc.*, 2009, **19**, 369–374.
- 21 *Radiative Decay Engineering*, ed. C. D. Geddes and J. R. Lakowicz, Springer, New York, 2004.
- 22 *Metal-enhanced fluorescence*, ed. C. D. Geddes, Wiley-Blackwell, Oxford, 2010.
- 23 P. J. Tarcha, J. DeSaja-Gonzalez, S. Rodriguez-Llorente and R. Aroca, *Appl. Spectrosc.*, 1999, **53**, 43–48.
- 24 O. G. Tovmachenko, C. Graf, D. J. van den Heuvel, A. van Blaaderen and H. C. Gerritsen, *Adv. Mater.*, 2006, **18**, 91–95.
- 25 Y. Chen, K. Munechika and D. S. Ginger, *Nano Lett.*, 2007, **7**, 690–696.
- 26 J. Kummerlen, A. Leitner, H. Brunner, F. R. Aussenegg and A. Wokaun, *Mol. Phys.*, 1993, **80**, 1031–1046.
- 27 Y. D. Jin and X. H. Gao, *Nat. Nanotechnol.*, 2009, **4**, 571–576.
- 28 D. M. Cheng and Q. H. Xu, *Chem. Commun.*, 2007, 248–250.
- 29 J. Malicka, I. Gryczynski, Z. Gryczynski and J. R. Lakowicz, *Anal. Biochem.*, 2003, **315**, 57–66.
- 30 K. Ray, R. Badugu and J. R. Lakowicz, *Chem. Mater.*, 2007, **19**, 5902–5909.
- 31 K. Ray, R. Badugu and J. R. Lakowicz, *Langmuir*, 2006, **22**, 8374–8378.
- 32 K. Ray, R. Badugu and J. R. Lakowicz, *J. Phys. Chem. C*, 2007, **111**, 7091–7097.
- 33 J. Zhang, Y. Fu, M. H. Chowdhury and J. R. Lakowicz, *J. Phys. Chem. C*, 2007, **111**, 11784–11792.
- 34 R. Aroca, G. J. Kovacs, C. A. Jennings, R. O. Loutfy and P. S. Vincett, *Langmuir*, 1988, **4**, 518–521.
- 35 W. L. Barnes, *J. Mod. Opt.*, 1998, **45**, 661–699.
- 36 R. L. Stoermer and C. D. Keating, *J. Am. Chem. Soc.*, 2006, **128**, 13243–13254.
- 37 K. Okamoto, I. Niki, A. Shvartser, Y. Narukawa, T. Mukai and A. Scherer, *Nat. Mater.*, 2004, **3**, 601–605.
- 38 G. R. Fleming, A. W. E. Knight, J. M. Morris, R. J. S. Morrison and G. W. Robinson, *J. Am. Chem. Soc.*, 1977, **99**, 4306–4311.
- 39 C. D. Geddes, *Meas. Sci. Technol.*, 2001, **12**, R53–R88.
- 40 B. D. Llewellyn, *Biotech. Histochem.*, 2009, **84**, 159–177.
- 41 E. Gurr, *Synthetic dyes in biology, medicine and chemistry*, Academic Press, London, 1971.
- 42 Y. Zhang, A. Dragan and C. D. Geddes, *J. Phys. Chem. C*, 2009, **113**, 12095–12100.
- 43 J. Zhang, Y. Fu and J. R. Lakowicz, *J. Phys. Chem. C*, 2009, **113**, 19404–19410.